



# Cyclopentadienyl molybdenum dicarbonyl $\eta^3$ -allyl complexes as catalyst precursors for olefin epoxidation. Crystal structures of $\text{Cp}'\text{Mo}(\text{CO})_2(\eta^3\text{-C}_3\text{H}_5)$ ( $\text{Cp}' = \eta^5\text{-C}_5\text{H}_4\text{Me}$ , $\eta^5\text{-C}_5\text{Me}_5$ )

Patrícia Neves<sup>a</sup>, Cláudia C.L. Pereira<sup>a,b</sup>, Filipe A. Almeida Paz<sup>a</sup>, Sandra Gago<sup>a</sup>, Martyn Pillinger<sup>a</sup>, Carlos M. Silva<sup>a</sup>, Anabela A. Valente<sup>a,\*</sup>, Carlos C. Romão<sup>c,d</sup>, Isabel S. Gonçalves<sup>a,\*</sup>

<sup>a</sup> Department of Chemistry, CICECO, University of Aveiro, 3810-193 Aveiro, Portugal

<sup>b</sup> Unit of Chemical and Radiopharmaceutical Sciences (UCRS), Nuclear and Technological Institute, Estrada Nacional 10, 2686-953 Sacavém, Portugal

<sup>c</sup> Instituto de Tecnologia Química e Biológica da Universidade Nova de Lisboa, Av. da República, Estação Agronómica Nacional, 2780-157 Oeiras, Portugal

<sup>d</sup> Alfama Ltd., Taguspark, Núcleo Central 267, 2740-122, Porto Salvo, Portugal

## ARTICLE INFO

### Article history:

Received 19 May 2010

Received in revised form

29 June 2010

Accepted 1 July 2010

Available online 5 August 2010

### Keywords:

Molybdenum

Cyclopentadienyl ligands

Oxidative decarbonylation

Homogeneous catalysis

Olefin epoxidation

## ABSTRACT

The complexes  $\text{Cp}'\text{Mo}(\text{CO})_2(\eta^3\text{-C}_3\text{H}_5)$  [ $\text{Cp}' = \eta^5\text{-C}_5\text{H}_5$  (**1**),  $\eta^5\text{-C}_5\text{H}_4\text{Me}$  (**2**),  $\eta^5\text{-C}_5\text{Me}_5$  (**3**)] have been prepared, structurally characterised by X-ray diffraction (**2**, **3**), and tested as catalyst precursors for the epoxidation of olefins at 55 °C. Complex **1** gave a turnover frequency (TOF) of 310 mol mol<sub>Mo</sub><sup>-1</sup> h<sup>-1</sup> in the epoxidation of *cis*-cyclooctene with *tert*-butylhydroperoxide (TBHP, in decane) as oxidant, and 1,2-epoxycyclooctane was obtained quantitatively within 6 h. A similar result was obtained for complex **2**, while the TOF for **3** was about one order of magnitude lower, suggesting a possible activity dependence on the ring substituents. For **1** the use of 1,2-dichloroethane as solvent increased the initial reaction rate to 361 mol mol<sub>Mo</sub><sup>-1</sup> h<sup>-1</sup>, with no decrease in epoxide selectivity. Under these conditions the reaction rates for other olefins increased in the order 1-octene < *trans*-2-octene < cyclododecene < (*R*)-(+)-limonene < *cis*-cyclooctene, and, with the exception of limonene, the corresponding epoxide was the only product. For **1** the selective epoxidation of *cis*-cyclooctene could also be achieved in aqueous solution, using TBHP or H<sub>2</sub>O<sub>2</sub> as oxidants, which gave epoxide yields of 99% and 27% at 24 h, respectively. The possibility of facilitating catalyst recycling by using ionic liquids as solvents was investigated.

© 2010 Elsevier B.V. All rights reserved.

## 1. Introduction

The allyl complexes  $\text{Cp}'\text{M}(\text{CO})_2(\eta^3\text{-C}_3\text{H}_5)$  [ $\text{Cp}' = \text{Cp}$  ( $\eta^5\text{-C}_5\text{H}_5$ ) or substituted Cp; M = Cr, Mo, W] have for some time been of considerable theoretical and experimental interest [1–6]. From a synthetic standpoint, these complexes serve as precursors to several mixed ring and indenyl analogues of molybdenocene and tungstenocene [5]. For example, protonation of  $\text{Cp}'\text{Mo}(\text{CO})_2(\eta^3\text{-C}_3\text{H}_5)$  with HBF<sub>4</sub> followed by cyclopentadiene coordination gives  $\eta^4$ -cyclopentadiene complexes. Compounds with the CpCp'Mo moiety are then available through oxidative, reductive, or photochemical pathways [5a,5b]. The Mo<sup>II</sup> allyl complexes are also useful in organic synthesis because functional groups adjacent to the  $\eta^3$ -allyl group can be transformed with excellent stereoselectivity and regioselectivity [6]. Another potential application concerns the use

of the  $\text{Cp}'\text{M}(\text{CO})_2(\eta^3\text{-C}_3\text{H}_5)$  moiety as a labelling group in bio-organometallic chemistry [7].

Since 2003 there has been growing interest in the use of molybdenum carbonyl complexes as precursors to Mo<sup>VI</sup> catalysts for oxidation reactions [8–13], with most of the research being focussed on tricarbonyl complexes [8,12,13]. The oxidative decarbonylation of  $\text{Cp}'\text{Mo}(\text{CO})_3\text{Cl}$  ( $\text{Cp}' = \eta^5\text{-C}_5\text{R}_5$ ; R = H, Me, CH<sub>2</sub>Ph) with excess *tert*-butylhydroperoxide (TBHP) in *n*-decane provides a convenient pathway to generating the dioxomolybdenum(VI) complexes  $\text{Cp}'\text{MoO}_2\text{Cl}$  [8a]. Like the isoelectronic derivatives with general formula  $\text{MoO}_2\text{X}_2\text{L}$  (X = Cl, Br, Me; L = bidentate Lewis base ligand), the  $\text{Cp}'\text{MoO}_2\text{X}$  complexes (X = Cl, alkyl) catalyse the epoxidation of olefins with TBHP as the oxidising agent [8a–8c,8h,8i,14,15]. With R = CH<sub>2</sub>Ph (Bz) the catalytic activity for *cis*-cyclooctene epoxidation at 55 °C surpassed that of the well-known  $\text{MeReO}_3/\text{H}_2\text{O}_2$  system. Similar catalytic results can be obtained by using the parent tricarbonyl complexes directly as catalyst precursors. Depending on the nature of X, R, and the reaction conditions, the Mo<sup>VI</sup> species formed by *in situ* oxidation may include  $\text{Cp}'\text{MoO}_2\text{X}$  and  $[\text{Cp}'\text{MoO}_2]_2(\mu\text{-O})$ , the peroxo complexes  $\text{Cp}'\text{MoO}(\text{O}_2)\text{X}$  and

\* Corresponding authors. Fax: +351 234 370084.

E-mail addresses: atav@ua.pt (A.A. Valente), igoncalves@ua.pt (I.S. Gonçalves).

[Cp'MoO(O<sub>2</sub>)<sub>2</sub>(μ-O)], and the anionic trioxo complex [Cp'MoO<sub>3</sub>]<sup>−</sup> [16]. Experimental and theoretical studies have indicated that the complexes activate TBHP for oxygen atom transfer to an olefin by forming a sterically crowded active intermediate containing a coordinated *tert*-butylperoxido ligand [8h,8l,15]. Molybdenum η<sup>3</sup>-allyl dicarbonyl complexes of the type [Mo(η<sup>3</sup>-allyl)X(CO)<sub>2</sub>L<sub>n</sub>] (X = Cl, Br; L = MeCN or bidentate diimine ligand) have also been examined as precursors to reactive epoxidation catalysts [9]. Oxido-bridged dimers of the type [MoO<sub>2</sub>(N–N)]<sub>2</sub>(μ-O)<sub>2</sub> were proposed as the active species.

As part of our ongoing research into molybdenum carbonyl complexes as precursors to oxomolybdenum(VI) catalysts, we now wish to report on the synthesis of the complexes Cp'Mo(CO)<sub>2</sub>(η<sup>3</sup>-C<sub>3</sub>H<sub>5</sub>) [Cp' = Cp, η<sup>5</sup>-C<sub>5</sub>H<sub>4</sub>Me (CpMe), η<sup>5</sup>-C<sub>5</sub>Me<sub>5</sub> (Cp\*)] (Chart 1) and their catalytic performance in the epoxidation of several olefins with TBHP or H<sub>2</sub>O<sub>2</sub> as oxidising agents. The X-ray crystal structures of the CpMe and Cp\* analogues are described.

## 2. Experimental

### 2.1. General considerations

All preparations and manipulations were carried out using standard Schlenk techniques under argon. Solvents were dried by standard procedures, distilled under argon, and kept over 4 Å molecular sieves. Microanalyses for CHN were performed at the ITQB, Oeiras, Portugal (by Z. Tavares). <sup>1</sup>H and <sup>13</sup>C NMR spectra were measured with a Bruker CXP 300 instrument. Chemical shifts are quoted in parts per million from tetramethylsilane. Infrared spectra were recorded on a Unicam Mattson Mod 7000 FTIR spectrophotometer using KBr pellets and/or in a CH<sub>2</sub>Cl<sub>2</sub> solution. The compounds (η<sup>3</sup>-C<sub>3</sub>H<sub>5</sub>)Mo(CO)<sub>2</sub>(NCMe)<sub>2</sub>Cl [17] and CpMo(CO)<sub>2</sub>(η<sup>3</sup>-C<sub>3</sub>H<sub>5</sub>) (**1**) [5b] were prepared as described in the literature.

### 2.2. General procedure for the preparation of Cp'Mo(CO)<sub>2</sub>(η<sup>3</sup>-C<sub>3</sub>H<sub>5</sub>) (Cp' = CpMe, Cp\*)

Solid (η<sup>3</sup>-C<sub>3</sub>H<sub>5</sub>)Mo(CO)<sub>2</sub>(NCMe)<sub>2</sub>Cl and LiCp' were weighed in a Schlenk tube and cooled to −80 °C. Precooled THF or toluene (30 mL) was added and the mixture was slowly warmed to room temperature. Stirring was continued for 18 h, after which time the solution was evaporated to dryness. The residue was extracted with hexane at 40 °C for a few hours. The resultant yellow extract solution was concentrated, and a yellow powder was separated, which was recrystallised from hexane/Et<sub>2</sub>O at −30 °C.

#### 2.2.1. (CpMe)Mo(CO)<sub>2</sub>(η<sup>3</sup>-C<sub>3</sub>H<sub>5</sub>) (**2**)

Reagents, solvent, yield: LiCpMe (0.55 g, 6.44 mmol), (η<sup>3</sup>-C<sub>3</sub>H<sub>5</sub>)Mo(CO)<sub>2</sub>(NCMe)<sub>2</sub>Cl (2.00 g, 6.44 mmol), THF, 88% (1.54 g). Anal. Calcd for C<sub>11</sub>H<sub>12</sub>MoO<sub>2</sub> (272.15): C, 48.55; H, 4.44. Found: C, 48.56; H,

4.49%. Selected FTIR (CH<sub>2</sub>Cl<sub>2</sub>, cm<sup>−1</sup>): 1944vs, 1858vs [ν(CO)]. <sup>1</sup>H NMR (CDCl<sub>3</sub>, 300 MHz, room temperature, δ ppm): 5.15 (s, 2H, C<sub>5</sub>H<sub>4</sub>Me), 5.09 (s, 2H, C<sub>5</sub>H<sub>4</sub>Me), 3.76 (m, 1H, allyl-H<sup>2</sup>), 2.66 (d, 2H, allyl-H<sup>1,3</sup>), 1.87 (s, 3H, Me), 0.93 (d, 2H, allyl-H<sup>1,3</sup>). <sup>13</sup>C NMR (CDCl<sub>3</sub>, 75 MHz, room temperature, δ ppm): 237.5 (CO), 92.7 (C<sub>5</sub>H<sub>4</sub>Me), 88.2 (C<sub>5</sub>H<sub>4</sub>Me), 69.2 (allyl-C<sup>2</sup>), 41.0 (allyl-C<sup>1,3</sup>), 13.5 (C<sub>5</sub>H<sub>4</sub>Me). The atom numbering of the allyl group for the NMR assignments is shown in Chart 1.

#### 2.2.2. Cp\*Mo(CO)<sub>2</sub>(η<sup>3</sup>-C<sub>3</sub>H<sub>5</sub>) (**3**)

Reagents, solvent, yield: LiCp\* (0.69 g, 4.83 mmol), (η<sup>3</sup>-C<sub>3</sub>H<sub>5</sub>)Mo(CO)<sub>2</sub>(NCMe)<sub>2</sub>Cl (1.50 g, 4.83 mmol), toluene, 58% (0.92 g). Anal. Calcd for C<sub>15</sub>H<sub>20</sub>MoO<sub>2</sub> (328.25): C, 54.88; H, 6.14. Found: C, 54.72; H, 6.00%. Selected FTIR (CH<sub>2</sub>Cl<sub>2</sub>, cm<sup>−1</sup>): 1933vs, 1846vs [ν(CO)]. <sup>1</sup>H NMR (CDCl<sub>3</sub>, 300 MHz, room temperature, δ ppm): 2.80 (m, 1H, allyl-H<sup>2</sup>), 2.12 (d, 2H, allyl-H<sup>1,3</sup>), 1.79 (s, 15H, Me), 0.90 (d, 2H, allyl-H<sup>1,3</sup>). <sup>13</sup>C NMR (CDCl<sub>3</sub>, 75 MHz, room temperature, δ ppm): 240.3 (CO), 103.4 (C<sub>5</sub>Me<sub>5</sub>), 75.3 (allyl-C<sup>2</sup>), 43.2 (allyl-C<sup>1,3</sup>), 10.5 (Me).

### 2.3. X-ray crystallography

Suitable single-crystals of **2** and **3** were manually harvested from the crystallisation vials and mounted on Hampton Research CryoLoops using FOMBLIN Y perfluoropolyether vacuum oil (LVAC 25/6) purchased from Aldrich with the help of a Stemi 2000 stereomicroscope equipped with Carl Zeiss lenses [18]. Data were collected on a Bruker X8 Kappa APEX II CCD area-detector diffractometer (Mo K<sub>α</sub> graphite-monochromated radiation, λ = 0.7107 Å) controlled by the APEX2 software package [19], and equipped with an Oxford Cryosystems Series 700 cryostream monitored remotely using the software interface Cryopad [20]. Images were processed using the software package SAINT+ [21], and data were corrected for absorption by the multi-scan semi-empirical method implemented in SADABS [22]. Structures were solved using the Patterson synthesis algorithm implemented in SHELXS-97 [23], which allowed the immediate location of the central molybdenum centre for each complex. All of the remaining non-hydrogen atoms were directly located from difference Fourier maps calculated from successive full-matrix least squares refinement cycles on F<sup>2</sup> using SHELXL-97 [24]. Non-hydrogen atoms were successfully refined using anisotropic displacement parameters.

Hydrogen atoms attached to carbon were located at their idealised positions using appropriate HFIX instructions in SHELXL: 43 for the aromatic hydrogen atoms associated with the Cp rings; 13 and 23 for the central and peripheral hydrogen atoms of the η<sup>3</sup>-allyl ligands; 137 for the substituent methyl group of CpMe, and 127 for the same groups belonging to Cp\*. These hydrogen atoms were included in subsequent refinement cycles in riding-motion approximation with isotropic thermal displacements parameters

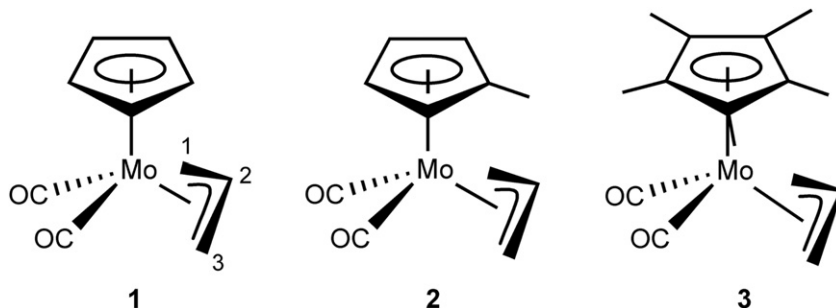


Chart 1.

( $U_{\text{iso}}$ ) fixed at 1.2 or 1.5 (only for the Me moieties) times  $U_{\text{eq}}$  of the attached carbon atom.

The last difference Fourier map synthesis showed, for **2**, the highest peak ( $0.263 \text{ e}\text{\AA}^{-3}$ ) and deepest hole ( $-0.272 \text{ e}\text{\AA}^{-3}$ ) located at  $0.50 \text{ \AA}$  from H(8) and  $0.32 \text{ \AA}$  from H(8) (both associated with the  $\eta^3$ -allyl ligand), respectively; for **3**, the highest peak ( $0.362 \text{ e}\text{\AA}^{-3}$ ) and deepest hole ( $-0.295 \text{ e}\text{\AA}^{-3}$ ) located at  $0.66 \text{ \AA}$  from C(6) and  $1.26 \text{ \AA}$  from H(9C) (both associated with the Cp\* ligand and located on the crystallographic mirror plane of space group Pnma), respectively. Information concerning crystallographic data collection and structure refinement details is summarised in Table 1.

#### 2.4. Catalytic olefin epoxidation

The liquid phase epoxidation of *cis*-cyclooctene was carried out at  $55 \text{ }^\circ\text{C}$  under air (atmospheric pressure) in a micro reaction vessel equipped with a magnetic stirrer and immersed in a thermostated oil bath. The micro vessel was loaded with the complex ( $36 \text{ }\mu\text{mol}$ ), olefin ( $3.6 \text{ mmol}$ ), oxidant ( $5.5 \text{ mmol}$  of either  $5.5 \text{ M}$  TBHP in decane,  $70\%$  aq. TBHP or  $30\%$  aq.  $\text{H}_2\text{O}_2$ ), and, optionally, 1,2-dichloroethane ( $2 \text{ mL}$ ) or a room temperature ionic liquid ( $100 \text{ }\mu\text{L}$ ). The TBHP/decane solution was used as received from Sigma–Aldrich and may contain up to  $4\%$  water. In the experiments with different olefins, 1,2-dichloroethane ( $2 \text{ mL}$ ) was used as solvent. Samples were withdrawn periodically and analysed using a Varian 3800 GC equipped with a capillary column (SPB-5,  $20 \text{ m} \times 0.25 \text{ mm} \times 0.25 \text{ }\mu\text{m}$ ) and a flame ionisation detector. Undecane was used as an internal standard added after the reaction.

**Table 1**  
Crystal and structure refinement data for (CpMe)Mo(CO) $_2$ ( $\eta^3$ -C $_3$ H $_5$ ) (**2**) and Cp\*Mo(CO) $_2$ ( $\eta^3$ -C $_3$ H $_5$ ) (**3**).

	<b>2</b>	<b>3</b>
Formula	C $_{11}$ H $_{12}$ MoO $_2$	C $_{15}$ H $_{20}$ MoO $_2$
Formula weight	272.15	328.25
Temperature (K)	150(2)	180(2)
Crystal system	Monoclinic	Orthorhombic
Space group	P2 $_1$ /n	Pnma
<i>a</i> (Å)	8.2649(5)	9.5295(7)
<i>b</i> (Å)	11.4169(7)	13.4922(9)
<i>c</i> (Å)	11.1609(6)	11.4888(7)
$\beta$ (°)	103.381(2)	–
Volume (Å $^3$ )	1024.55(10)	1477.16(17)
<i>Z</i>	4	4
$D_c$ (g cm $^{-3}$ )	1.764	1.476
$\mu$ (Mo-K $\alpha$ ) (mm $^{-1}$ )	1.249	0.880
$F(000)$	544	672
Crystal size (mm)	$0.26 \times 0.08 \times 0.08$	$0.30 \times 0.06 \times 0.01$
Crystal type	Yellow blocks	Yellow needles
$\theta$ range	$3.57$ – $25.35$	$3.55$ – $25.34$
Index ranges	$-9 \leq h \leq 9$ $-13 \leq k \leq 13$ $-13 \leq l \leq 13$	$-10 \leq h \leq 11$ $-16 \leq k \leq 16$ $-13 \leq l \leq 13$
Reflections collected	29069	23397
Independent reflections	1861 ( $R_{\text{int}} = 0.0308$ )	1397 ( $R_{\text{int}} = 0.0499$ )
Data completeness	99.3%	99.4%
Data/parameters	1861/128	1397/91
Final <i>R</i> indices [ $I > 2\sigma(I)$ ] <sup>a,b</sup>	$R1 = 0.0139$ , $wR2 = 0.0329$	$R1 = 0.0263$ , $wR2 = 0.0549$
Final <i>R</i> indices (all data) <sup>a,b</sup>	$R1 = 0.0157$ , $wR2 = 0.0338$	$R1 = 0.0380$ , $wR2 = 0.0593$
Weighting scheme <sup>c</sup>	$m = 0.0128$ , $n = 0.7356$	$m = 0.0199$ , $n = 2.1687$
Largest diff. peak and hole	$0.263$ and $-0.272 \text{ e}\text{\AA}^{-3}$	$0.362$ and $-0.295 \text{ e}\text{\AA}^{-3}$

$$^a R1 = \sum ||F_o| - |F_c|| / \sum |F_o|.$$

$$^b wR2 = \sqrt{\sum [w(F_o^2 - F_c^2)]^2 / \sum [w(F_o^2)]^2}.$$

$$^c w = 1/[\sigma^2(F_o^2) + (mP)^2 + nP] \quad \text{where } P = (F_o^2 + 2F_c^2)/3.$$

To recover and reuse the ionic liquid-standing catalysts, the reaction mixtures after the first run were cooled to room temperature, *n*-hexane ( $1 \text{ mL}$ ) was added, and the mixtures stirred for ca.  $5 \text{ min}$ , followed by centrifugation to enhance the separation of the two liquid phases. The colourless, transparent, upper phase consisting of hexane/olefin/products was separated from the IL + catalyst phase. The IL phase was extracted twice more with hexane, and the complete removal of reagent/products was confirmed by GC analysis. A second run was initiated by adding substrate and oxidant in equimolar amounts to those charged in the first run, and monitoring the reaction carried out at  $55 \text{ }^\circ\text{C}$  for  $24 \text{ h}$ .

### 3. Results and discussion

#### 3.1. Synthesis and characterisation of the $\eta^3$ -allyl dicarbonyl complexes

The reaction of ( $\eta^3$ -C $_3$ H $_5$ )Mo(CO) $_2$ (NCMe) $_2$ Cl with the lithium salt of cyclopentadiene (Cp) or methylcyclopentadiene (CpMe) in THF gives the complexes CpMo(CO) $_2$ ( $\eta^3$ -C $_3$ H $_5$ ) (**1**) and (CpMe)Mo(CO) $_2$ ( $\eta^3$ -C $_3$ H $_5$ ) (**2**) in  $80$ – $90\%$  yield. When the same reaction is carried out using the lithium salt of pentamethylcyclopentadiene (Cp\*), the yield of the desired  $\eta^3$ -allyl dicarbonyl complex (**3**) is much lower, but can be improved to  $58\%$  by using toluene as the solvent instead of THF. Complexes **1**–**3** (Chart 1) are bright-yellow solids, which are moderately air stable and may be stored unchanged for long periods under nitrogen. They are very soluble in polar solvents such as CH $_2$ Cl $_2$  and ethanol, and also in non-polar solvents such as *n*-hexane and diethyl ether. As expected, the IR spectra of the complexes show a pair of carbonyl stretching bands between ca.  $1845$  and  $1950 \text{ cm}^{-1}$ . The stretching frequencies for dichloromethane solutions follow the order **1** ( $1859, 1946 \text{ cm}^{-1}$ )  $\approx$  **2** ( $1858, 1944 \text{ cm}^{-1}$ )  $>$  **3** ( $1846, 1933 \text{ cm}^{-1}$ ). The lower  $\nu(\text{CO})$  for complex **3** can be explained by the higher donor capacity of the Cp\* ligand, *i.e.*, the substitution of the hydrogen atoms in Cp and CpMe by methyl groups (Cp\*) increases the electron density at the metal, which results in greater  $\pi$  back-bonding to the carbonyl groups and hence a lower C–O bond order. At room temperature the solution  $^1\text{H}$  NMR spectra reveal only one set of signals for the allyl ligands, presumably due to rapid *exo*–*endo* interconversion on the NMR time scale. The complex ( $\eta^5$ -C $_5$ H $_4$ SiMe $_3$ )Mo(CO) $_2$ ( $\eta^3$ -C $_3$ H $_5$ ) exhibits similar temperature-dependent dynamic behaviour in solution [25].

The structures of **2** and **3** were determined by X-ray crystallography (Fig. 1 and Table 2). While complex **3** is rigorously symmetric, having a crystallographic mirror plane bisecting the O=C–Mo–C=O angle (and consequently the  $\eta^5$ -Cp\* and  $\eta^3$ -allyl ligands, see Fig. 1b), this is not the case for **2**. Indeed, even though the complex (CpMe)Mo(CO) $_2$ ( $\eta^3$ -C $_3$ H $_5$ ) could, in theory, exhibit the same kind of crystallographic symmetry as that registered for **3**, the  $\eta^5$ -CpMe ligand is rotated by approximately  $27^\circ$  along the axis containing its centre of gravity ( $C_{g,\text{Cp}}$ ) and the molybdenum centre (Fig. 1a), ultimately leading to an overall reduction in both local and crystallographic symmetries. The isolation of this conformational isomer can be rationalised by taking into account the supramolecular interactions mediating the crystal packing of **2** (see Discussion below).

The molybdenum centres in complexes **2** and **3** are coordinated to two carbonyl (C=O) groups, one methylcyclopentadienyl ring (for **2**) or one pentamethylcyclopentadienyl ring (for **3**), and one allyl ligand (Fig. 1). Even though the structures of a considerable number of molybdenum dicarbonyl–allyl complexes containing a Cp' aromatic ring have been reported [7,26], those which most resemble **2** and **3** were described in the 1980s: CpMo(CO) $_2$ ( $\eta^3$ -C $_3$ H $_5$ ) by Fallor et al. [27], and (AcCp)Mo(CO) $_2$ ( $\eta^3$ -C $_3$ H $_5$ ) (Ac = acetyl) by Vanarsdale and Kochi [28]. Besides the striking similarities concerning the molybdenum coordination spheres, the allyl ligands in

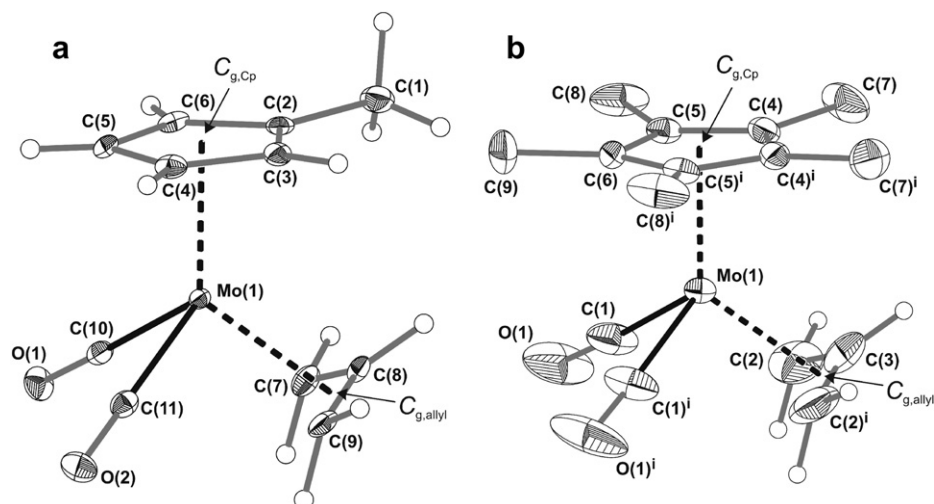


**Fig. 1.** Schematic representation of the molecular units present in the crystal structures of (a)  $(\text{CpMe})\text{Mo}(\text{CO})_2(\eta^3\text{-C}_3\text{H}_5)$  (**2**) and (b)  $\text{Cp}^*\text{Mo}(\text{CO})_2(\eta^3\text{-C}_3\text{H}_5)$  (**3**) showing the labelling scheme for all non-hydrogen atoms. Thermal ellipsoids are drawn at the 30% probability level and hydrogen atoms are represented as small spheres with arbitrary radii (those belonging to the  $\text{Cp}^*$  ligand in complex **3** have been omitted). Mo–C bonds to the  $\eta^5\text{-CpMe}$ ,  $\eta^5\text{-Cp}^*$  and  $\eta^3\text{-allyl}$  ligands have been replaced by black-filled dashed bonds to the corresponding centres of gravity ( $C_{g,\text{Cp}}$  and  $C_{g,\text{allyl}}$ , respectively). For selected bond lengths and angles see Table 2. Symmetry transformation used to generate equivalent atoms: (i)  $x, 1.5 - y, z$ .

all four crystal structures are coordinated via a typical *exo* conformation, further substantiating the assumptions of Faller and co-workers that this isomer is the most energetically favourable in the solid state [17,27]. The average dihedral angles between the mean planes containing the  $\eta^3\text{-allyl}$  groups and the  $\eta^5\text{-Cp}$ -substituted rings are approximately identical and calculated as ca.  $34.2^\circ$  for **2** and ca.  $35.0^\circ$  for **3**.

The observed Mo–C distances for the coordinated  $\text{Cp}'$  and allyl groups are typical of  $\eta^5$  and  $\eta^3$  coordination modes, respectively, as revealed by systematic searches in the Cambridge Structural Database (CSD, Version 5.31, November 2009 [29]) for geometrical data on similar structural arrangements. For the substituted Cp

rings the Mo–C bond lengths were found in the ranges of 2.2982(16)–2.4077(16) Å for **2** and 2.296(4)–2.379(2) Å for **3** (Table 2), which are in agreement with the values reported for related materials (data from the CSD: CpMe, 152 entries, range 2.15–2.53 Å with median of 2.38 Å; Cp\*, 394 entries, range 2.03–2.53 Å with median 2.36 Å). The Mo–C bond lengths with the  $\eta^3\text{-allyl}$  groups were found in the ranges of 2.2261(16)–2.3427(17) Å for **2** and 2.202(5)–2.321(3) Å for **3**, which, once again, are well within the expected interval (141 entries in the CSD with values between 2.13 and 2.39 Å, median of 2.22 Å). As generally encountered for complexes with a geometry resembling a three-legged piano-stool, the Mo–C distances with the CpMe group clearly indicate a slight “slip” from the expected  $\eta^5$ -coordination mode toward a  $\eta^3$ -type, with the Mo–C(2,3) bond lengths of **2** being statistically longer (Fig. 1 and Table 2). This structural feature registered for **2** (but not **3**) can be rationalised by taking into account that, on the one hand, the  $\text{Cp}^*$  moiety has local pseudo- $C_5$  symmetry and, consequently, the effect of steric repulsion is evenly distributed across the five carbon atoms of the ring and, on the other hand, the methyl substituent of CpMe is closer to C(2) and C(3). The Mo–C bond lengths with the C=O groups were found in the range of 1.928(3)–1.9554(17) (Table 2), and are consistent with the values reported for related molybdenum-containing structures (3709 entries in the CSD, range 1.48–2.37 Å with median of 1.98 Å). Taking into account the absence of structurally significant interactions directly involving these coordinated carbonyl groups (see the Discussion below about the intermolecular interactions mediating the crystal packing of individual complexes), it is noteworthy that the geometries of the Mo–C≡O bonds are clearly different for the two complexes: while in **2** the  $\angle[\text{Mo}(1)\text{--C}(10,11)\text{--O}(1,2)]$  interaction angles are almost linear [ $178.1(1)^\circ$  and  $179.7(1)^\circ$ ], in **3** the  $\angle[\text{Mo}(1)\text{--C}(1)\text{--O}(1)]$  of the crystallographically independent connection deviates from linearity [ $176.8(1)^\circ$ ]. These structural differences arise from the steric hindrance created by the proximity of the  $\eta^3\text{-allyl}$  group which is, on average, closer to the C≡O groups in **3**.

By replacing the aforementioned Mo–C bonds to each organic ligand by a single connection to the corresponding centres of gravity ( $C_{g,\text{Cp}}$  and  $C_{g,\text{allyl}}$ ), the overall coordination geometries of molybdenum can be envisaged as highly distorted tetrahedrons, typical of the class of three-legged piano-stool complexes to which

**Table 2**

Selected bond lengths (Å) and angles ( $^\circ$ ) for the molybdenum coordination environments present in compounds **2** and **3**.<sup>a,b,c</sup>

$(\text{CpMe})\text{Mo}(\text{CO})_2(\eta^3\text{-C}_3\text{H}_5)$ ( <b>2</b> )			
Mo(1)–C(2)	2.4077(16)	$C_{g,\text{Cp}}\text{--Mo}(1)\text{--C}(10)$	120.65(6)
Mo(1)–C(3)	2.3812(16)	$C_{g,\text{Cp}}\text{--Mo}(1)\text{--C}(11)$	122.54(6)
Mo(1)–C(4)	2.3263(16)	$C_{g,\text{Cp}}\cdots\text{Mo}(1)\cdots C_{g,\text{allyl}}$	126.33(6)
Mo(1)–C(5)	2.2982(16)	C(10)–Mo(1)–C(11)	79.68(7)
Mo(1)–C(6)	2.3364(16)	C(10)–Mo(1)– $C_{g,\text{allyl}}$	99.72(6)
Mo(1)–C(7)	2.3427(17)	C(11)–Mo(1)– $C_{g,\text{allyl}}$	96.60(6)
Mo(1)–C(8)	2.2261(16)		
Mo(1)–C(9)	2.3293(17)		
Mo(1)–C(10)	1.9554(17)		
Mo(1)–C(11)	1.9423(18)		
Mo(1)⋯ $C_{g,\text{Cp}}$	2.0185(1)		
Mo(1)⋯ $C_{g,\text{allyl}}$	2.0488(1)		
$\text{Cp}^*\text{Mo}(\text{CO})_2(\eta^3\text{-C}_3\text{H}_5)$ ( <b>3</b> )			
Mo(1)–C(1)	1.928(3)	$C_{g,\text{Cp}}\text{--Mo}(1)\text{--C}(1)$	120.13(2)
Mo(1)–C(2)	2.321(3)	$C_{g,\text{Cp}}\cdots\text{Mo}(1)\cdots C_{g,\text{allyl}}$	127.05(2)
Mo(1)–C(3)	2.202(5)	C(1)–Mo(1)–C(1) <sup>i</sup>	82.2(2)
Mo(1)–C(4)	2.379(2)	C(1)–Mo(1)– $C_{g,\text{allyl}}$	98.41(2)
Mo(1)–C(5)	2.327(3)		
Mo(1)–C(6)	2.296(4)		
Mo(1)⋯ $C_{g,\text{Cp}}$	2.008(1)		
Mo(1)⋯ $C_{g,\text{allyl}}$	2.035(1)		

<sup>a</sup>  $C_{g,\text{Cp}}$  – centroid of the coordinated  $\eta^5\text{-CpMe}$  and  $\eta^5\text{-Cp}^*$  aromatic rings [C(2)–C(6) and C(4)–C(6) for **2** and **3**, respectively].

<sup>b</sup>  $C_{g,\text{allyl}}$  – centroid of the coordinated  $\eta^3\text{-allyl}$  ligands [C(7)–C(9) and C(2)–C(3) for **2** and **3**, respectively].

<sup>c</sup> Symmetry transformation used to generate equivalent atoms: (i)  $x, 1.5 - y, z$ .

these compounds belong. Even though the bond distances are, for each compound, all approximately identical [found in the ranges of 1.9423(18)–2.049(1) Å for **2** and 1.928(3)–2.035(1) Å for **3**], the internal tetrahedral angles clearly reflect the different chemical moieties coordinated to these metal centres, ranging from 79.68(7)° to 126.33(6)° for **2**, and from 82.2(2)° to 127.05(2)° for **3** (Table 2). Nevertheless, the C–Mo–(C<sub>g,allyl</sub>) basal angles for the two complexes are approximately identical, ranging from 79.68(7)° to 99.72(6)° for **2**, and from 82.2(2)° to 98.41(2)° for **3** (Fig. 1 and Table 2). Notably, the different internal tetrahedral angles mentioned above are also intimately related with the steric strain imposed in each individual complex by the coordination of the Cp' ligands. Since Cp\* is clearly sterically more hindered than CpMe, the average distance in **3** between the former moiety and the coordinated allyl group tends to be slightly longer, leading to a larger C<sub>g,Cp</sub>···Mo···C<sub>g,allyl</sub> angle (Fig. 1 and Table 2). As a result, and in order to minimise the repulsion between the moieties composing the coordination sphere of molybdenum, the coordinated C≡O groups in **3** tend to be farther apart, which leads to a larger O≡C–Mo–C≡O angle.

The complexes (CpMe)Mo(CO)<sub>2</sub>(η<sup>3</sup>-C<sub>3</sub>H<sub>5</sub>) interact in the crystal structure of **2** via two moderately strong [*d*(C···C<sub>g,Cp</sub>) of 3.563(1) Å

and <(CHC<sub>g,Cp</sub>) of ca. 149°] but cooperative C–H···π interactions involving the methyl substituent of one complex and the aromatic ring of another (Fig. 2a). These interactions lead to the formation of a supramolecular centrosymmetric dimer which close packs in a parallel fashion in the *ab* plane of the unit cell (Fig. 2b). In the crystal structure of **3** no significant supramolecular interactions could be found between neighbouring Cp\*Mo(CO)<sub>2</sub>(η<sup>3</sup>-C<sub>3</sub>H<sub>5</sub>) complexes with the packing being essentially driven by the need to effectively fill the space. Also, in **3** individual complexes self-organise into layers but in this case their relative orientation is typical of a herringbone tiling (Fig. 3a); layers close pack in the unit cell in a typical ABAB··· fashion along the [001] direction (Fig. 3b).

### 3.2. Olefin epoxidation

Complexes **1**, **2** and **3** were investigated as catalyst precursors for the epoxidation of *cis*-cyclooctene, used as a model substrate for unfunctionalised olefins, with TBHP as oxidant and without co-solvent (other than the decane present in the oxidant solution), under atmospheric air at 55 °C. Whereas in the absence of a metal complex (but with TBHP) or of TBHP (but with metal complex) olefin conversion was negligible, in the presence of complexes **1–3**

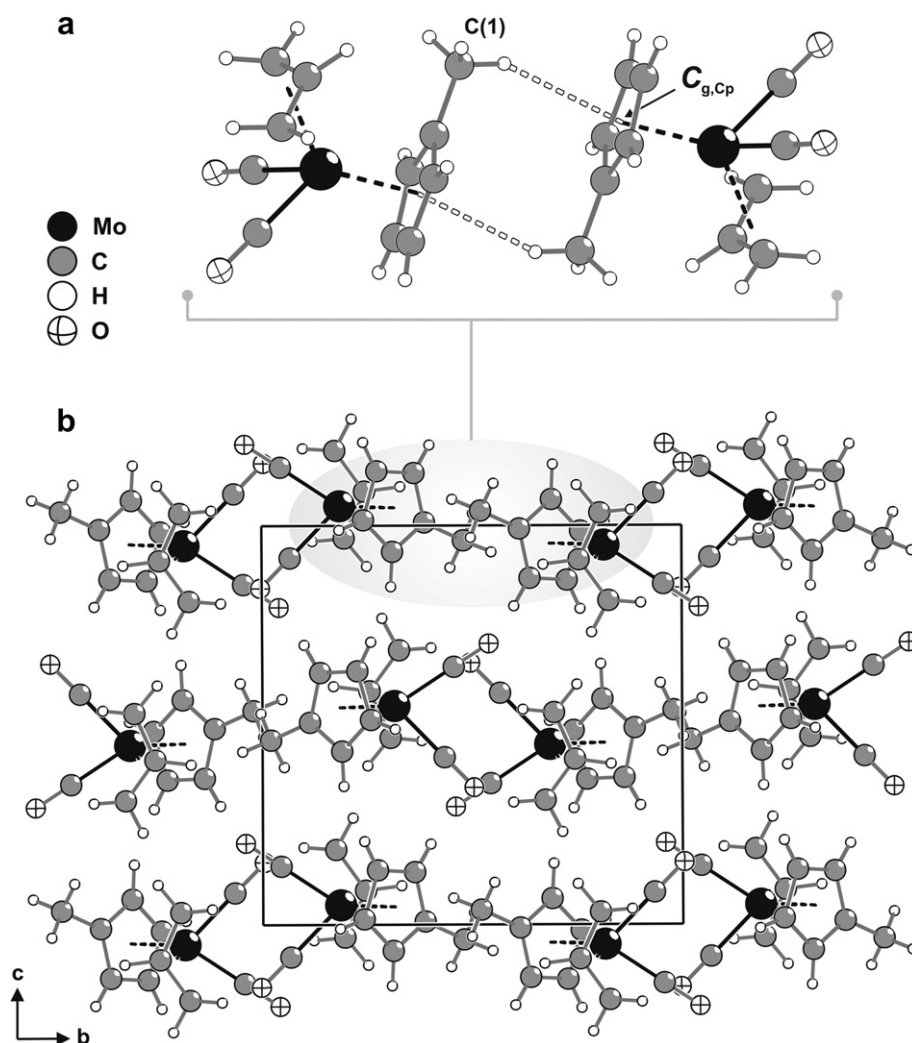


**Fig. 2.** (a) Schematic representation of the cooperative C–H···π interactions (dashed white-filled bonds) between coordinated η<sup>5</sup>-CpMe moieties belonging to adjacent (CpMe)Mo(CO)<sub>2</sub>(η<sup>3</sup>-C<sub>3</sub>H<sub>5</sub>) complexes in **2**: C(1)–H(1A)···C<sub>g,Cp</sub> with *d*(C···C<sub>g,Cp</sub>) of 3.563(1) Å and <(CHC<sub>g,Cp</sub>) of ca. 149°. (b) Crystal packing of compound **2** viewed along the [100] direction of the unit cell. Mo–C bonds to the η<sup>5</sup>-CpMe and η<sup>3</sup>-allyl ligands have been replaced by black-filled dashed bonds to the corresponding centres of gravity (C<sub>g,Cp</sub> and C<sub>g,allyl</sub>, respectively). Symmetry transformation used to generate equivalent atoms: (i) –*x*, 1 – *y*, 2 – *z*.

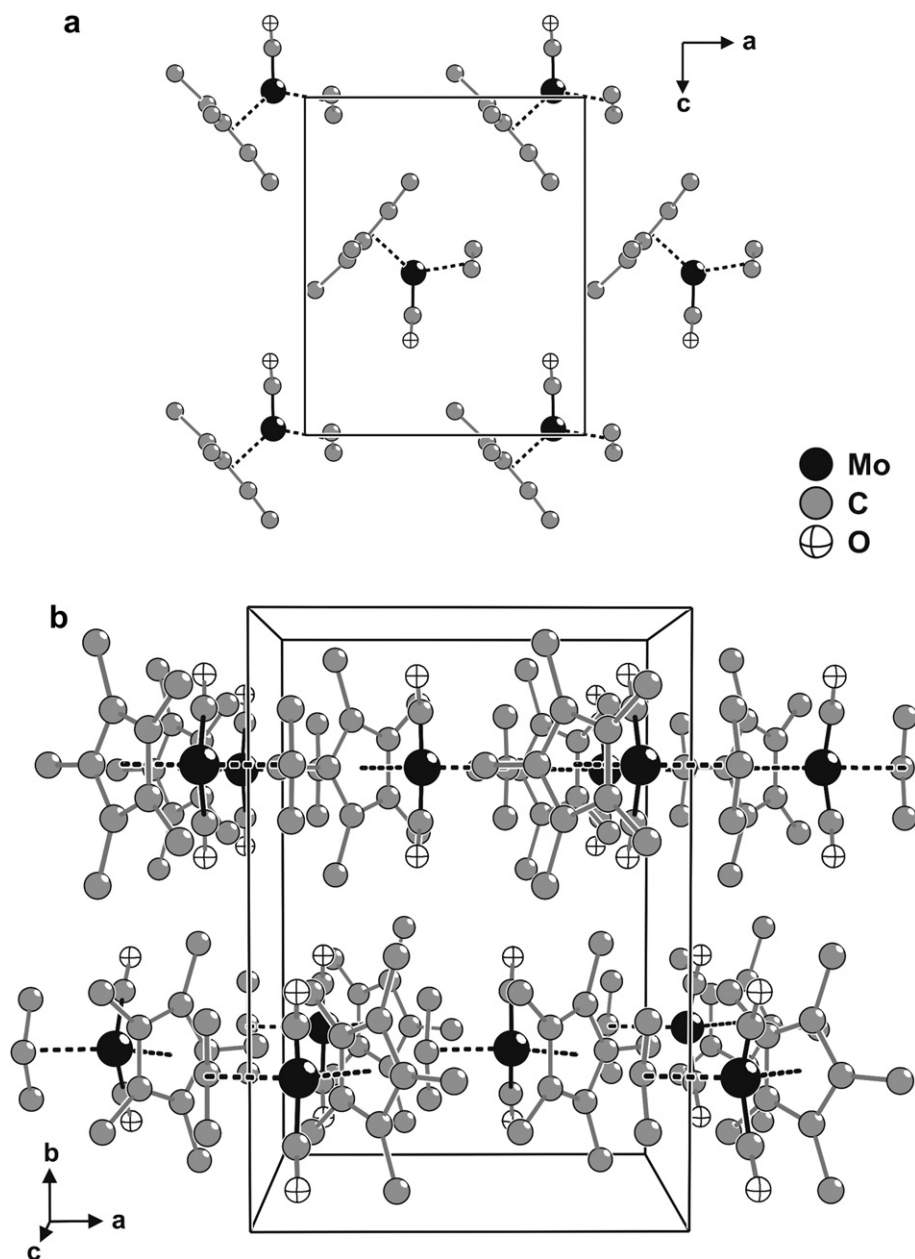


**Fig. 3.** (a) Herringbone-type parallel packing of individual  $\text{Cp}^*\text{Mo}(\text{CO})_2(\eta^3\text{-C}_3\text{H}_5)$  complexes, which leads to the formation of a layer placed in the  $ac$  plane of the unit cell of **3**. (b) Crystal packing of compound **3** viewed in perspective along the  $[001]$  direction of the unit cell. Hydrogen atoms have been omitted for clarity and Mo–C bonds to the  $\eta^5\text{-Cp}^*$  and  $\eta^3\text{-allyl}$  ligands have been replaced by black-filled dashed bonds to the corresponding centres of gravity ( $C_{g,\text{Cp}}$  and  $C_{g,\text{allyl}}$ , respectively).

**Table 3**

*cis*-Cyclooctene epoxidation with TBHP (in decane) at 55 °C using molybdenum carbonyl complexes as catalyst precursors, without a co-solvent (unless otherwise specified).

Catalyst precursor	TOF <sup>a</sup> ( $\text{mol mol}_{\text{Mo}}^{-1} \text{h}^{-1}$ )	Conversion <sup>b</sup> (%)		Selectivity <sup>b</sup> (%)	
		Run 1	Run 2	Run 1	Run 2
<b>1</b>	310	99/100	84/99	100/100	100/100
<b>2</b>	307	94/98	67/89	100/100	100/100
<b>3</b>	32	50/84	53/86	93/96	98/98
$\text{CpMo}(\text{CO})_3\text{Cl}$	499	99/100	85/100	100/100	100/100
$\text{CpMo}(\text{CO})_3\text{Me}^c$	248	96/100	82/97	100/100	100/100
$\text{CpMo}(\text{CO})_3\text{Me}/$ $[\text{BMIM}]\text{BF}_4^c$	121 (14) <sup>c</sup>	86/98	44/89	100/100	100/100

<sup>a</sup> Turnover frequency calculated at ca. 10 min.

<sup>b</sup> *cis*-Cyclooctene conversion and epoxide selectivity at 6/24 h for runs 1 and 2.

<sup>c</sup> Published in ref. [8j]; values in brackets refer to run 2.

and TBHP, conversion reached 84–100% at 24 h (Table 3). For **1** and **2** the epoxide was the only product, while **3** gave 1,2-cyclooctanediol as a minor by-product (possibly indicating the formation of metal species with enhanced Lewis acidity, which may favour epoxide ring opening). These results indicate that the metal complex is required for the activation of the oxidant and that the oxidant is required for the formation of active species responsible for oxygen atom transfer to the olefin. For comparison, the epoxidation of *cis*-cyclooctene was carried out using  $\text{CpMo}(\text{CO})_3\text{Cl}$  (Table 3), under similar reaction conditions, which gave a somewhat higher turnover frequency ( $\text{TOF} = 499 \text{ mol mol}_{\text{Mo}}^{-1} \text{h}^{-1}$ ) than that observed for **1** ( $310 \text{ mol mol}_{\text{Mo}}^{-1} \text{h}^{-1}$ ), and the epoxide yield was nearly quantitative within 20 min (Fig. 4). The TOFs for **1** and **2** are comparable to those found for  $\text{CpMo}(\text{CO})_3\text{Me}$  [8j] (Table 3) and

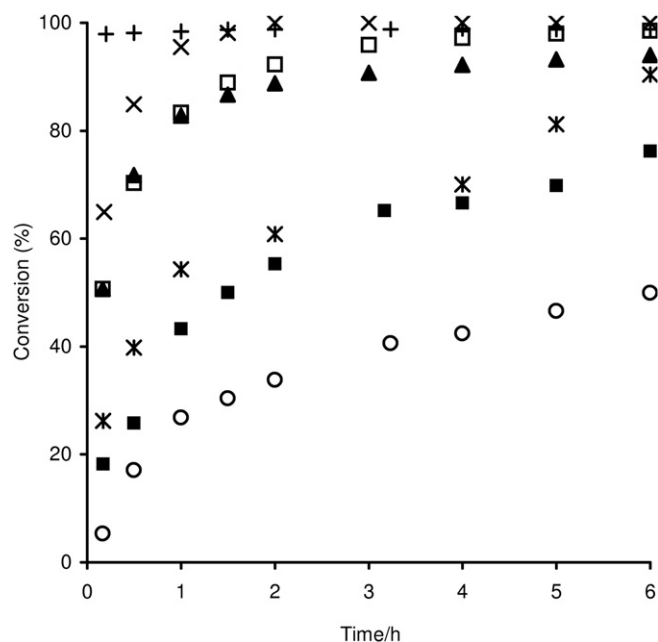


**Fig. 4.** Kinetic profiles of *cis*-cyclooctene epoxidation with TBHP (in decane) at 55 °C using molybdenum carbonyl complexes as catalyst precursors and, unless otherwise stated, no co-solvent: **1** (□); **2** (▲); **3** (○); CpMo(CO)<sub>3</sub>Cl (+); **1** + 1,2-dichloroethane (×); **1** + [BMIM]BF<sub>4</sub> (\*); **1** + [BMPy]BF<sub>4</sub> (■).

some of the most active MoO<sub>2</sub>X<sub>2</sub>L complexes used as catalysts for the same reaction under similar conditions [30].

The kinetic profiles for **1–3** are similar in that there is a rapid rise in conversion during the first hour or so, with no induction period being observed, followed by a more gradual increase as the reaction proceeds (Fig. 4). This behaviour, which is also typical of the tricarbonyl complexes Cp'Mo(CO)<sub>3</sub>X [8], suggests that the active oxidising species are formed within the first few minutes of reaction, and, possibly, that the initial rate of olefin epoxidation is not significantly limited by the oxidative decarbonylation of the precursor complex. The TOF for **3** is about one order of magnitude lower than that for **1** and **2**, and this activity difference is maintained throughout the 24 h of reaction. Previous studies with Cp'Mo

**Table 4**

Olefin epoxidation at 55 °C using CpMo(CO)<sub>2</sub>(η<sup>3</sup>-C<sub>3</sub>H<sub>5</sub>) (**1**) as the catalyst precursor.

Olefin	Oxidant	Solvent	TOF <sup>a</sup> (mol mol <sub>Mo</sub> <sup>-1</sup> h <sup>-1</sup> )	Conv. <sup>b</sup> (%)	Select. <sup>b</sup> (%)
<i>cis</i> -Cyclooctene	TBHP aq.	None	97	80/99	100/100
	H <sub>2</sub> O <sub>2</sub> aq.	None	<1	11/27	100/100
	TBHP (decane)	None	310	99/100	100/100
		DCE	361	100/100	100/100
1-Octene	TBHP (decane)	[BMIM]BF <sub>4</sub>	156	90/94	100/100
		[BMPy]BF <sub>4</sub>	108	76/93	100/100
			(57) <sup>c</sup>	(64/87) <sup>c</sup>	(100/100) <sup>c</sup>
			(36) <sup>c</sup>	(50/70) <sup>c</sup>	(100/95) <sup>c</sup>
1-Octene	TBHP (decane)	DCE	6	35/51	100/100
<i>trans</i> -2-Octene	TBHP (decane)	DCE	81	74/89	100/100
Cyclododecene	TBHP (decane)	DCE	188	86/92	100/100
( <i>R</i> )-(+)-Limonene	TBHP (decane)	DCE	289	98/100	79/70 <sup>d</sup>

<sup>a</sup> Turnover frequency calculated at ca. 10 min.

<sup>b</sup> Olefin conversion and epoxide selectivity at 6/24 h.

<sup>c</sup> Information relative to the second run.

<sup>d</sup> Sum of selectivities to 1,2-epoxy-*p*-menth-8-ene and 1,2,8,9-diepoxy-*p*-menthane. At 24 h, the molar ratio epoxide/diepoxy was 1.2.

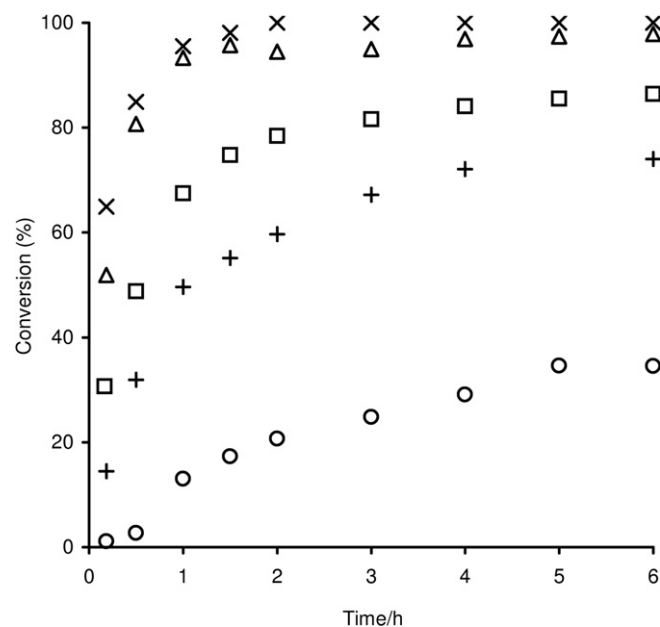
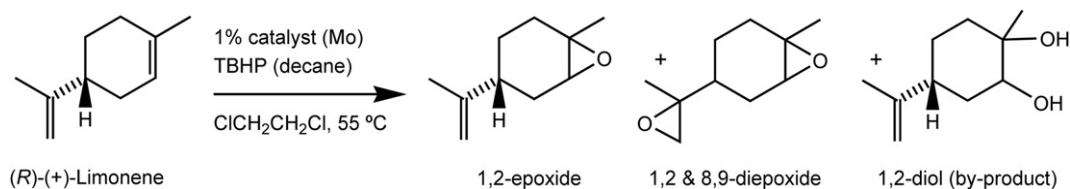


**Fig. 5.** Kinetic profiles for the conversion of olefins with TBHP (in decane) at 55 °C using complex **1** as the catalyst precursor: *cis*-cyclooctene (×), (*R*)-(+)-limonene (Δ), cyclododecene (□), *trans*-2-octene (+) and 1-octene (○).

(CO)<sub>3</sub>Me (Cp' = Cp or Cp\*) used as catalyst precursors for the same reaction revealed a similar activity difference [8d], which suggested that the cyclopentadienyl ligands were retained during the *in situ* oxidative decarbonylation to give the Mo<sup>VI</sup> catalysts, *i.e.*, that steric and/or electronic effects involving the Cp' ring strongly influenced the overall performance of the catalysts [8f]. Modifying Cp' in the precursor complexes **1–3** may change the nature of the oxomolybdenum species formed *in situ* by oxidation. In an effort to get some insight into the nature of such species, the catalytic reaction using *cis*-cyclooctene, TBHP and **1** was scaled up by a factor of 10 and allowed to run for 6 h at 55 °C. After cooling to room temperature, a small amount of manganese dioxide was added to destroy the excess of TBHP, and the mixture was filtered. Evaporation of the filtrate under reduced pressure gave an intractable yellow oil which we were unable to purify and characterise. Based on the previous work with the complexes Cp'Mo(CO)<sub>3</sub>X (see the Introduction, section 1) and the well-known chemistry of Cp'Mo(CO)<sub>2</sub>(η<sup>3</sup>-C<sub>3</sub>H<sub>5</sub>), we may expect that the dicarbonyl complexes **1–3** will lose the allyl and CO groups upon reaction with TBHP. The products may include bimetallic systems like [Cp'MoO<sub>2</sub>]<sub>2</sub>(μ-O), as found for the oxidation of (η<sup>5</sup>-C<sub>5</sub>Bz<sub>5</sub>)Mo(CO)<sub>3</sub>Me [8f], as well as their corresponding peroxo species or the anionic complex [Cp'MoO<sub>3</sub>]<sup>-</sup>.

To assess the stability of the catalytic systems derived from complexes **1–3** and, for comparison, CpMo(CO)<sub>3</sub>Cl, two consecutive 24 h runs were carried out by recharging the micro reactor after the first 24 h run with *cis*-cyclooctene and TBHP in the same amounts as those used initially, and monitoring the reaction for a further 24 h, at 55 °C. For **1** and **3** the catalytic results at 6/24 h are roughly the same for runs 1 and 2 (Table 3). The results for **1** are comparable to those observed for CpMo(CO)<sub>3</sub>Cl, as well as to those found for CpMo(CO)<sub>3</sub>Me used as a catalyst precursor under similar reaction conditions [8j]. In the case of **2** the reaction is slower in the second run, which may be due to the formation of different metal species.

In an effort to facilitate catalyst recycling with complex **1** as the precursor, the ionic liquids (ILs) 1-butyl-3-methylimidazolium tetrafluoroborate ([BMIM]BF<sub>4</sub>) and 1-butyl-4-methylpyridinium tetrafluoroborate ([BMPy]BF<sub>4</sub>) were used, which are both readily available and inexpensive. Under the reaction conditions used



**Scheme 1.** Limonene and its oxidation products.

liquid–liquid biphasic mixtures were obtained comprising a colourless organic phase containing *cis*-cyclooctene and decane, and a denser, clear yellow IL phase containing the oxidant and the fully dissolved metal species. Control experiments performed with IL but without metal complex gave 36% and 27% conversion at 24 h for [BMIM]BF<sub>4</sub> and [BMPy]BF<sub>4</sub>, with epoxide yields of 31% and 24%, respectively. For the catalytic systems **1** + IL, the epoxide was obtained as the only reaction product in ca. 94% yield at 24 h (Table 4). The kinetic profiles are quite similar (Fig. 4); the TOF was slightly higher for [BMIM]BF<sub>4</sub> than for [BMPy]BF<sub>4</sub> (156 and 108 mol mol<sub>Mo</sub><sup>-1</sup> h<sup>-1</sup>, respectively, Table 4). The results for complex **1** + [BMIM]BF<sub>4</sub> are somewhat comparable to those reported for the [BMIM]BF<sub>4</sub>–standing CpMo(CO)<sub>3</sub>Me (Tables 3 and 4) [8j]. The reactions performed with the ILs are significantly slower than those involving a single liquid phase, which may be due to mass transfer limitations [8j].

When the catalyst + IL systems were recycled (see Section 2.4 for details about the hexane extraction procedure used to recover the catalyst + IL phase), the reaction of the olefin in the second run was somewhat slower than that in the first run, and epoxide selectivity decreased slightly in the case of [BMPy]BF<sub>4</sub>. To check whether active metal species were extracted during the work-up procedure, the three *n*-hexane fractions resulting from the extraction of the catalyst + [BMPy]BF<sub>4</sub> system were combined, and the volatiles were evaporated under reduced pressure, giving a yellowish oily residue. *cis*-Cyclooctene and TBHP were added to the residue in the same amounts as those charged for the first run, without co-solvent, and the mixture was stirred during 6 h at 55 °C. Conversion at 6 h was 59%, which is quite significant compared to the 99% conversion observed for complex **1** without solvent (Table 3). Hence, the *n*-hexane fractions contained active metal species, explaining the lower reaction rates for the recycled catalyst + IL systems. This drawback has been reported for several related molybdenum complex/IL catalytic systems, occurring within the first couple of batch runs [8j, 31]. Somewhat more efficient molybdenum complex/IL catalytic systems (stable during at least two batch runs) include [MoO<sub>2</sub>Cl(HC(bim)<sub>3</sub>)]Cl/[BMIM]PF<sub>6</sub> or [BMPy]PF<sub>6</sub> [32], where HC(bim)<sub>3</sub> = tris(benzimidazolyl)methane, and [MoO<sub>2</sub>L]Na/[BMIM]NTf<sub>2</sub> [33], where L is a Schiff base and NTf<sub>2</sub> = anionic bis{(trifluoromethyl)sulfonyl}amide. It is desirable to choose an immiscible IL-extraction solvent pair which favours high partition ratios of the catalyst in the IL and of the target product in the extraction solvent; otherwise further work-up procedures for purification of the target products may be required. On the other hand, distillation of the target product may be an attractive alternative to solvent extraction but its feasibility will depend on the thermal stability and vapour pressures of the different compounds of the reaction mixture.

Compared with the results obtained using **1** as the catalyst precursor and no additional solvent (other than the decane present in the oxidant solution), the catalytic performance improved in terms of initial reaction rate (TOF = 361 mol mol<sub>Mo</sub><sup>-1</sup> h<sup>-1</sup>) by addition of 1,2-dichloroethane (DCE) as solvent, with no decrease in epoxide selectivity (Table 4, Fig. 4). The dilution of the reaction mixture,

which might have been expected to give a lower TOF, was apparently offset by the favourable polarity of the reaction medium (e.g., readily dissolving and/or stabilising metal species). The catalytic performance of **1** was further investigated for the epoxidation of other unfunctionalised olefins, namely 1-octene, *trans*-2-octene, cyclododecene and (*R*)-(+)-limonene, using DCE as solvent, at 55 °C (Table 4, Fig. 5). With the exception of limonene, the corresponding epoxide was always the only observed product. In the reaction of limonene, 1,2-epoxy-*p*-menth-8-ene and 1,2-8,9-diepoxyp-menthane were the main products (70% epoxide yield at 24 h), and the corresponding 1,2-diol was a by-product (Scheme 1). The catalytic epoxidation is regioselective, occurring preferentially at the endocyclic double bond rather than at the exocyclic one. When the reaction was carried out at 35 °C, the total epoxide yield at 24 h increased to 76%. The reaction rates for the studied olefins increased in the following order (at 55 °C): 1-octene < *trans*-2-octene < cyclododecene < (*R*)-(+)-limonene < *cis*-cyclooctene. Hence, electron-rich olefins such as *cis*-cyclooctene display a greater reactivity than electron deficient olefins such as 1-octene. This probably reflects the electrophilic nature of the oxygen atom transfer from the active intermediate to the olefinic double bond. Comparing the two cyclic olefins, the lower reactivity of cyclododecene may be attributed to steric hindrance being more significant in the formation of the transition state of the epoxidation, leading to a slower epoxidation reaction.

To study the activity of these systems in aqueous solution, TBHP or H<sub>2</sub>O<sub>2</sub> were used as oxidants in *cis*-cyclooctene epoxidation with complex **1** as the catalyst precursor (Table 4). The reaction mixtures consisted of two immiscible liquid phases, *i.e.*, an organic phase containing *cis*-cyclooctene and cyclooctene oxide, and an aqueous phase containing the oxidant and molybdenum species. With 70% aq. TBHP the initial reaction rate (97 mol mol<sub>Mo</sub><sup>-1</sup> h<sup>-1</sup>) was lower than that measured for the decane solution of TBHP (310 mol mol<sub>Mo</sub><sup>-1</sup> h<sup>-1</sup>), but after 24 h practically the same conversion was reached, giving 99% epoxide yield. Under similar conditions, the catalyst precursor CpMo(CO)<sub>3</sub>Cl gave a TOF of 108 mol mol<sub>Mo</sub><sup>-1</sup> h<sup>-1</sup> and an epoxide yield of 80% at 24 h [16]. The reaction of *cis*-cyclooctene with **1** as the precursor and 30% aq. H<sub>2</sub>O<sub>2</sub> as the oxidant was very sluggish (27% conversion at 24 h), although the epoxide was the only product. Nevertheless, these results are an improvement over those obtained with the complexes CpMo(CO)<sub>3</sub>Cl, Cp\*MoO<sub>2</sub>Cl and [Cp\*MoO<sub>2</sub>]<sub>2</sub>(μ-O), which are unable to activate aqueous H<sub>2</sub>O<sub>2</sub> for *cis*-cyclooctene epoxidation [8d,8f,16].

#### 4. Conclusions

The present work has demonstrated that complexes of the type Cp'Mo(CO)<sub>2</sub>(η<sup>3</sup>-C<sub>3</sub>H<sub>5</sub>) are potentially interesting as a new class of molybdenum carbonyl precursors to olefin epoxidation catalysts. The stability of these catalytic systems seems fair, based on the catalyst reuse tests. The poorer performance (slower reaction) of the Cp\* analogue indicates some dependence of catalytic performance on the ring substituents. In the future, *in situ* spectroscopic measurements of the reaction of the precursors with the oxidant

may help to elucidate the nature of the molybdenum species formed.

## Acknowledgements

We are grateful to the Fundação para a Ciência e a Tecnologia (FCT, Portugal), POCI 2010, OE and FEDER for funding through the project with ref. no. PTDC/QUI/71198/2006. CICECO is acknowledged for financial support through the project entitled "Metal carbonyl intercalated anion exchangers as drug delivery systems". The FCT is thanked for grants to PN, CCLP and SG, and for financial support toward the purchase of the single-crystal diffractometer.

## Appendix A. Supplementary material

CCDC-777390 (2) and CCDC-777391 (3) contain the supplementary crystallographic data (excluding structure factors) for this paper. These data can be obtained free of charge from The Cambridge Crystallographic Data Centre via [www.ccdc.cam.ac.uk/datarequest/cif](http://www.ccdc.cam.ac.uk/datarequest/cif).

## References

- (a) R.B. King, *Inorg. Chem.* 5 (1966) 2242–2243;  
(b) A. Davison, W.C. Rode, *Inorg. Chem.* 6 (1967) 2124–2125;  
(c) J.W. Faller, M.J. Incorvia, *Inorg. Chem.* 7 (1968) 840–842;  
(d) M. Cousins, M.L.H. Green, *J. Chem. Soc.* (1963) 889–894.
- D.W. Norman, M.J. Ferguson, J.M. Stryker, *Organometallics* 23 (2004) 2015–2019.
- (a) C. Limberg, A.J. Downs, T.M. Greene, T. Wistuba, *Eur. J. Inorg. Chem.* (2001) 2613–2618;  
(b) T.E. Bitterwolf, J.T. Bays, B. Scallorn, C.A. Weiss, M.W. George, I.G. Virrels, J.C. Linehan, C.R. Yonker, *Eur. J. Inorg. Chem.* (2001) 2619–2624.
- A. Ariafard, S. Bi, Z. Lin, *Organometallics* 24 (2005) 2241–2244.
- (a) J.R. Ascenso, C.G. de Azevedo, I.S. Gonçalves, E. Herdtweck, D.S. Moreno, C.C. Romão, J. Zühlke, *Organometallics* 13 (1994) 429–431;  
(b) J.R. Ascenso, C.G. de Azevedo, I.S. Gonçalves, E. Herdtweck, D.S. Moreno, M. Pessanha, C.C. Romão, *Organometallics* 14 (1995) 3901–3919;  
(c) I.S. Gonçalves, C.C. Romão, *J. Organomet. Chem.* 486 (1995) 155–161;  
(d) I.S. Gonçalves, P. Ribeiro-Claro, C.C. Romão, B. Royo, Z.M. Tavares, *J. Organomet. Chem.* 648 (2002) 270–279;  
(e) J. Honzík, A. Mukhopadhyay, T. Santos-Silva, M.J. Romão, C.C. Romão, *Organometallics* 28 (2009) 2871–2879;  
(f) J. Honzík, A. Mukhopadhyay, C. Bonifacio, C.C. Romão, *J. Organomet. Chem.* 695 (2010) 680–686.
- (a) C.-L. Li, R.-S. Liu, *Chem. Rev.* 100 (2000) 3127–3161 (and references cited therein);  
(b) A. Alcudia, R.G. Arrayás, L.S. Liebeskind, *J. Org. Chem.* 67 (2002) 5773–5778 (and references cited therein).
- D.R. van Staveren, T. Weyhermüller, N. Metzler-Nolte, *Organometallics* 19 (2000) 3730–3735.
- (a) M. Abrantes, A.M. Santos, J. Mink, F.E. Kühn, C.C. Romão, *Organometallics* 22 (2003) 2112–2118;  
(b) C. Freund, M. Abrantes, F.E. Kühn, *J. Organomet. Chem.* 691 (2006) 3718–3729 (and references cited therein);  
(c) F.E. Kühn, A.M. Santos, M. Abrantes, *Chem. Rev.* 106 (2006) 2455–2475 (references cited therein);  
(d) J. Zhao, A.M. Santos, E. Herdtweck, F.E. Kühn, *J. Mol. Catal. A: Chem.* 222 (2004) 265–271;  
(e) A.A. Valente, J.D. Seixas, I.S. Gonçalves, M. Abrantes, M. Pillinger, C.C. Romão, *Catal. Lett.* 101 (2005) 127–130;  
(f) A.M. Martins, C.C. Romão, M. Abrantes, M.C. Azevedo, J. Cui, A.R. Dias, M.T. Duarte, M.A. Lemos, T. Lourenço, R. Poli, *Organometallics* 24 (2005) 2582–2589;  
(g) A. Capapé, A. Raith, F.E. Kühn, *Adv. Synth. Catal.* 351 (2009) 66–70;  
(h) A.M. Al-Ajlouni, D. Veljanovski, A. Capapé, J. Zhao, E. Herdtweck, M.J. Calhorda, F.E. Kühn, *Organometallics* 28 (2009) 639–645;  
(i) M. Abrantes, F.A.A. Paz, A.A. Valente, C.C.L. Pereira, S. Gago, A.E. Rodrigues, J. Klinowski, M. Pillinger, I.S. Gonçalves, *J. Organomet. Chem.* 694 (2009) 1826–1833;  
(j) M. Abrantes, P. Neves, M.M. Antunes, S. Gago, F.A.A. Paz, A.E. Rodrigues, M. Pillinger, I.S. Gonçalves, C.M. Silva, A.A. Valente, *J. Mol. Catal. A: Chem.* 320 (2010) 19–26;  
(k) A. Capapé, A. Raith, E. Herdtweck, M. Cokoja, F.E. Kühn, *Adv. Synth. Catal.* 351 (2010) 547–556;  
(l) P.J. Costa, M.J. Calhorda, F.E. Kühn, *Organometallics* 29 (2010) 303–311.
- J.C. Alonso, P. Neves, M.J.P. da Silva, S. Quintal, P.D. Vaz, C. Silva, A.A. Valente, P. Ferreira, M.J. Calhorda, V. Félix, M.G.B. Drew, *Organometallics* 26 (2007) 5548–5556.
- V.V.K.M. Kandepi, A.P. da Costa, E. Peris, B. Royo, *Organometallics* 28 (2009) 4544–4549.
- T.R. Amarante, P. Neves, A.C. Coelho, S. Gago, A.A. Valente, F.A.A. Paz, M. Pillinger, I.S. Gonçalves, *Organometallics* 29 (2010) 883–892.
- C.A. Gamelas, T. Lourenço, A.P. da Costa, A.L. Simplicio, B. Royo, C.C. Romão, *Tetrahedron Lett.* 49 (2008) 4708–4712.
- A.V. Biradar, M.K. Dongare, S.B. Umbarkar, *Tetrahedron Lett.* 50 (2009) 2885–2888.
- M.K. Trost, R.G. Bergman, *Organometallics* 10 (1991) 1172–1178.
- A. Comas-Vives, A. Lledós, R. Poli, *Chem. Eur. J.* 16 (2010) 2147–2158.
- S.S. Balula, A.C. Coelho, S.S. Braga, A. Hazell, A.A. Valente, M. Pillinger, J.D. Seixas, C.C. Romão, I.S. Gonçalves, *Organometallics* 26 (2007) 6857–6863.
- J.W. Faller, C.-C. Chen, M.J. Mattina, A. Jakubowski, *J. Organomet. Chem.* 52 (1973) 361–386.
- T. Kottke, D. Stalke, *J. Appl. Crystallogr.* 26 (1993) 615.
- APEX2, Data Collection Software (Version 2.1-RC13). Bruker AXS, Delft, The Netherlands, 2006.
- Cryopad, Remote Monitoring and Control (Version 1.451). Oxford Cryosystems, Oxford, UK, 2006.
- SAINT+, Data Integration Engine (Version 7.23a). Bruker AXS, Madison, WI, USA, 2005.
- G.M. Sheldrick, SADABS Version 2.01, Bruker/Siemens Area Detector Absorption Correction Program. Bruker AXS, Madison, Wisconsin, USA, 1998.
- G.M. Sheldrick, SHELXS-97, Program for Crystal Structure Solution. University of Göttingen, Göttingen, Germany, 1997.
- G.M. Sheldrick, SHELXL-97, Program for Crystal Structure Refinement. University of Göttingen, Göttingen, Germany, 1997.
- S.S. Braga, I.S. Gonçalves, A.D. Lopes, M. Pillinger, J. Rocha, C.C. Romão, J.J.C. Teixeira-Dias, *J. Chem. Soc. Dalton Trans.* (2000) 2964–2968.
- (a) C.J. Beddows, M.R. Box, C. Butters, N. Carr, M. Green, M. Kursawe, M.F. Mahon, *J. Organomet. Chem.* 550 (1998) 267–282;  
(b) M. Green, T.D. McGrath, R.L. Thomas, A.P. Walker, *J. Organomet. Chem.* 532 (1997) 61–70;  
(c) L.C.F. Chao, H.K. Gupta, D.W. Hughes, J.F. Britten, S.S. Rigby, A.D. Bain, M.J. McGlinchey, *Organometallics* 14 (1995) 1139–1151;  
(d) S. Wan, M.J. Begley, P. Mountford, *J. Organomet. Chem.* 489 (1995) C28–C31;  
(e) M.-F. Liao, G.-H. Lee, S.-M. Peng, R.-S. Liu, *Organometallics* 13 (1994) 4973–4977;  
(f) J.W. Faller, Y. Ma, *Organometallics* 12 (1993) 1927–1930;  
(g) W.-J. Vong, S.-M. Peng, S.-H. Lin, W.-J. Lin, R.-S. Liu, *J. Am. Chem. Soc.* 113 (1991) 573–582;  
(h) N.W. Murrall, A.J. Welch, *Acta Crystallogr. Sect. C: Cryst. Struct. Commun.* 40 (1984) 401–403.
- J.W. Faller, D.F. Chodosh, D. Katahira, *J. Organomet. Chem.* 187 (1980) 227–231.
- W.E. Vanarsdale, J.K. Kochi, *J. Organomet. Chem.* 317 (1986) 215–232.
- (a) F.H. Allen, *Acta Crystallogr. Sect. B. Struct. Sci.* 58 (2002) 380–388;  
(b) F.H. Allen, W.D.S. Motherwell, *Acta Crystallogr. Sect. B. Struct. Sci.* 58 (2002) 407–422.
- (a) S.M. Bruno, J.A. Fernandes, L.S. Martins, I.S. Gonçalves, M. Pillinger, P. Ribeiro-Claro, J. Rocha, A.A. Valente, *Catal. Today* 114 (2006) 263–271;  
(b) S.M. Bruno, C.C.L. Pereira, M.S. Balula, M. Nolasco, A.A. Valente, A. Hazell, M. Pillinger, P. Ribeiro-Claro, I.S. Gonçalves, *J. Mol. Catal. A: Chem.* 261 (2007) 79–87.
- (a) A.A. Valente, Z. Petrovski, L.C. Branco, C.A.M. Afonso, M. Pillinger, A.D. Lopes, C.C. Romão, C.D. Nunes, I.S. Gonçalves, *J. Mol. Catal. A: Chem.* 218 (2004) 5–11;  
(b) F.E. Kühn, J. Zhao, M. Abrantes, W. Sun, C.A.M. Afonso, L.C. Branco, I.S. Gonçalves, M. Pillinger, C.C. Romão, *Tetrahedron Lett.* 46 (2005) 47–52.
- S. Gago, S.S. Balula, S. Figueiredo, A.D. Lopes, A.A. Valente, M. Pillinger, I.S. Gonçalves, *Appl. Catal. A. Gen.* 372 (2010) 67–72.
- C. Bibal, J.-C. Daran, S. Deroover, R. Poli, *Polyhedron* 29 (2010) 639–647.